Research Paper

Application of 1-D and 2-D Discrete Wavelet Transform to Crack Identification in Statically and Dynamically Loaded Plates

Anna KNITTER-PIĄTKOWSKA*, Michał GUMINIAK

Institute of Structural Analysis
Poznan University of Technology

Piotrowo 5, 60-965 Poznań, Poland
e-mail: michal.guminiak@put.poznan.pl
*Corresponding Author e-mail: anna.knitter-piatkowska@put.poznan.pl

The paper presents the problem of damage detection in thin plates while considering the influence of static and dynamic characteristics, especially with regard to the modes of vibration as well as the excitation by static loads. The problem of Kirchhoff plate bending is described and solved by the Boundary Element Method (BEM). Rectangular plates supported on boundary or plates supported on boundary and resting on the internal columns are examined. A defect is introduced by the additional edges forming a crack in the plate domain. The analyses of static and dynamic structural responses are carried out with the use of Discrete Wavelet Transform (DWT). Signal decomposition according to the Mallat pyramid algorithm is applied. To obtain a more adequate input function subjected to DWT the white noise disturbing the signal is considered together with the structural response. In the dynamic experiments the plate undergoes vibrations similar to natural modes. The measured variables are static deflections and vertical displacement amplitudes. All of them are established at internal collocation points distributed alongside the line parallel to selected plate edge.

Key words: damage detection; Kirchhoff plates; Boundary Element Method; Discrete Wavelet Transform.

1. INTRODUCTION

The presented work is dedicated to defects localization, provided that they exist, in the plate structure. This problem has been investigated by many authors, who presented some approaches allowing to locate a damaged part of a structure. MRÓZ and GARSTECKI proposed in [1] conditions of optimal loading for designing and identification of the structures. DEMS and MRÓZ described localization of damage in beams and plates by introducing a parameter dependent on frequency changes [2]. Heat transfer and inverse analysis were the base of the

response signals for ZIOPAJA, POZORSKI and GARSTECKI [3], BOUMECHRA [4] as well as KNITTER-PIĄTKOWSKA and GARBOWSKI [5], respectively. The signal processing method, namely wavelet transformation (WT) [6] also in its discrete form (DWT) [7] can be a very useful tool to localization and detection of defects. WT and especially DWT can properly indicate parts of a structure in which damage is possible to exist, wherein the information about undamaged structure is not necessary to perform the analysis of the response signal. A general review of the methods used for structural health monitoring (SHM) and damage detections has been presented by AN *et al.* [8].

The proposed numerical analysis is carried out while using static or dynamic signal responses of the structure. The plate bending is described and solved by the Boundary Element Method (BEM) in direct and modified form proposed by GUMINIAK [9, 10]. Rectangular plates supported on boundary and resting on internal column supports are considered. Defects are modelled as the slots near the plate boundary and introduced as additional free edges. Vertical displacements are taken into consideration as a structural response. In statics, the surface of deflection (2-D decomposition of the response signal) is analysed, for dynamics – the deflection line parallel to one of the boundaries and consistent with the selected mode of vibration is examined (1-D decomposition of the response signal). Decomposition of the response signal is carried out using DWT with Daubechies 4, 6, 8, Coiflet 6 and B-spline 1 families of wavelets. The problem of damage detection in plates supported on boundary and inside its domain has been described in detail and illustrated e.g. in the work [11]. This paper is the extension of earlier works [7, 11, 12] in which only one-dimensional DWT was applied.

2. THEORETICAL CONSIDERATION ON DISCRETE WAVELET TRANSFORM

Below, the basic assumptions of DWT for 1-D and 2-D analysis of signal will be briefly presented. The theory of the wavelet transformation (WT) was presented in many papers, e.g. [13].

Let the function $\psi(t)$, called the wavelet function (mother function), be continuous and belong to the field of $L^2(\mathbb{R})$. Additionally, the function $\psi(t)$ must satisfy the condition of admissibility [12]. The mother function may be real or complex-valued. The real-valued wavelets will be applied in the considered cases. For signal decomposition the set of wavelets (wavelet family) is needed. This set of functions is obtained by translating and scaling the function ψ what can be written by means of the relation:

(2.1)
$$\psi_{a,b} = \frac{1}{\sqrt{|a|}} \psi \left(\frac{t-b}{a} \right),$$

where t denotes a time or space coordinate, a is the scale parameter and b translation parameter. The parameters a and b take real values ($a, b \in (\mathbb{R})$) and additionally $a \neq 0$. The element $|a|^{-1/2}$ expresses the scale factor which ensures the constant wavelet energy regardless of the scale, it means i.e. $\|\psi_{a,b}\| = \|\psi\| = 1$.

In the current analysis of plate bending, Discrete Wavelet Transform (DWT) plays the leading role. For this approach, the wavelet family can be obtained by substitution $a = 1/2^j$ and $b = k/2^j$ in the Eq. (2.1) what leads to the following relation [12]:

$$(2.2) \qquad \psi_{j,k}(t) = 2^{(j/2)} \psi \left(2^j t - k\right),$$

in which k and j are scale and translation parameters, respectively. The interpretation of these parameters for the simplest Haar wavelet is illustrated e.g. in [15].

The Discrete Wavelet Transformation (DWT) is expressed by the equation [14]

$$(2.3) \qquad Wf(j,k) = 2^{j/2} \int\limits_{-\infty}^{\infty} f(t)\psi\left(2^j t - k\right) \, \mathrm{d}t = \langle f(t), \, \psi_{j,k} \rangle,$$

where $f(t)$ is the transformed response signal.

The scalar product of the response signal $f(t)$ and the wavelet function allows one to find the set of wavelet coefficients $d_{j,k} = \langle f(t), \, \psi_{j,k} \rangle$ therefore enables the discrete signal to be represented in the form of the combination of linear wavelet functions $\psi_{j,k}$ with wavelet coefficients $d_{j,k}$:

$$(2.4) \qquad f(t) = \sum_{j=0}^{J-1} \sum_{k} d_{j,k} \psi_{j,k}(t),$$

wherein the number of discrete values (number of input data) is 2^J.

To perform the multi-resolution analysis the scaling wavelet function (father function) $\varphi_{j,k}(t)$ is needed, which has the form

$$(2.5) \qquad \varphi_{j,k}(t) = 2^{j/2} \varphi\left(2^j t - k\right).$$

The scaling function $\varphi_{j,k}(t)$ should limit the unit area and has the unit energy. It fulfils the orthogonality and the translation conditions as well. This leads to the following relations respectively

$$(2.6) \qquad \int\limits_{-\infty}^{\infty} \varphi(t) \, \mathrm{d}t = 1,$$

$$(2.7) \qquad \langle \varphi(t), \varphi(t) \rangle = \int_{-\infty}^{\infty} |\varphi(t)|^2 \, dt = 1,$$

$$(2.8) \qquad \langle \varphi(t), \varphi(t-n) \rangle = 0, \qquad n \neq 0.$$

The function $f(t)$ is developed in series using the basic (mother) function $\psi(t)$ and the scaling (father) function $\varphi(t)$ [14]

$$(2.9) \qquad f(t) = \sum_{k=-\infty}^{\infty} a_{j,k} \varphi_{j,k}(t) + \sum_{k=-\infty}^{\infty} \sum_{j=0}^{\infty} d_{j,k} \psi_{j,k}(t),$$

where $a_{j,k}$ are the coefficients of the scaling wavelet, which are determined as follows

$$(2.10) \qquad a_{j,k} = \langle f(t), \varphi_{j,k} \rangle.$$

The wavelet $\psi(t)$ has a band-pass character, therefore coefficients $d_{j,k}$ contain information about higher frequencies, i.e. details and coefficients $a_{j,k}$ contain low pass information with a constant component. Its result is a signal approximation.

For 1-D analysis, the discrete signal decomposition can be written according to the Mallat pyramid algorithm in the form [13]:

$$(2.11) \qquad f_J = S_J + D_J + ... + D_n + ... + D_1, \qquad n = J - j,$$

where each component in signal representation is associated with a specific range of frequency and provides information at the scale level ($j = 1, ..., J$). The discrete parameter J describes the level of a multi-resolution analysis (MRA), S_J is the smooth signal representation, D_n and S_n are the details- and rough- parts of the signal and D_1 corresponds to the most detailed representation of the signal.
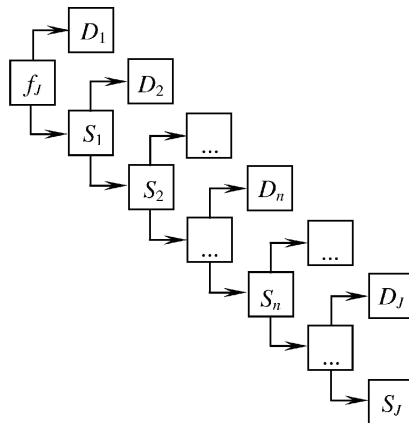

Fig. 1. Mallat pyramid algorithm for 1-D analysis.

To fulfil the dyadic requirements of DWT the function f_J must be approximated by $N = 2^J$ discrete values. The multi-resolution 1-D analysis according to the Mallat pyramid algorithm is illustrated in Fig. 1 and e.g. in papers [11–14]. In the current analysis of the defect detection, Daubechies, Coiflet and B-spline sets of wavelets will be applied. These families of wavelets are orthogonal, continuous and have a compact support.

For the 2-D analysis of the signal the Mallat pyramid algorithm has the following form [13]:

$$(2.12) \qquad F(x,y) = S_J(x,y) + \sum_{j=1}^{J} D_j^V(x,y) + \sum_{j=1}^{J} D_j^H(x,y) + \sum_{j=1}^{J} D_j^D(x,y),$$

where $S_J(x,y)$ is a smooth signal representation, $D_j^V(x,y)$, $D_j^H(x,y)$ and $D_j^D(x,y)$ are details and rough parts of the signal respectively, j is the level of decomposition and J is the level of MRA. The multi-resolution 2-D analysis according to the Mallat pyramid algorithm is illustrated in Fig. 2.
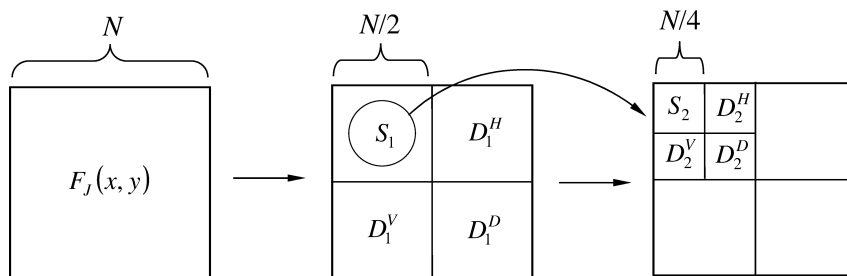

FIG. 2. Mallat pyramid algorithm for 2-D analysis.

For the dynamic analysis the sets of Daubechies 4 and 8 wavelets with 1-D procedure of DWT will be applied. In the static analysis the set of Coiflet 4 together with 2-D procedure of DWT and B-spline 1 wavelet will be used. In the dynamic analysis the sets of B-spline 1, Daubechies 5 and Coiflet 6 together with 2-D procedure of DWT and B-spline 1 wavelet will be used. Daubechies wavelets are asymmetrical and Coiflet wavelets are nearly symmetric. Both types have sharp edges and do not require a large number of coefficients hence they are often applied to solve a broad range of problems e.g. image analysis or defect detection. The order of Daubechies wavelet family functions is in the range of even numbers between 2 and 20. The Coiflet family of functions accepts the even integers 6, 12, 18, 24, and 30. The Daubechies wavelet of the second order corresponds to the simplest Haar wavelet. Basic and scaling functions of Daubechies 4 and Coilflet 6 wavelets are presented in Fig. 3.
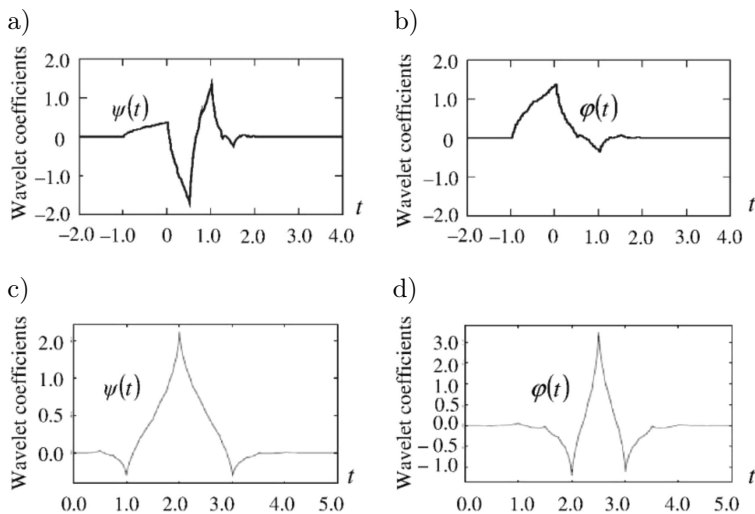
FIG. 3. Basis function (mother): a) Daubechies 4, c) Coiflet 6 wavelet and scaling function (father), b) Daubechies 4, and d) Coiflet 6 wavelet.

3. INTRODUCTION OF MEASUREMENT ERRORS IN NUMERICAL DATA

Measurement (observational) error is the difference between the measured value of quantity and its true value [16]. The measurement errors are an inevitable element of any real experiment and may be caused e.g. by measuring devices or methods, miscalculations or the influence of the environment on the previously mentioned causes. The example of a randomly generated error signal as a white noise is illustrated in Fig. 4 [12].
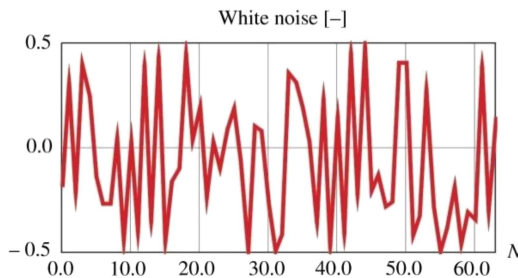

FIG. 4. White noise, values from -0.5 to 0.5.

To investigate the efficiency of DWT in damage detection during computer simulations, white noise was added to the signal. To adjust the scale of the inaccuracy to the intensity of the analysed response signal of the structure, white noise has been multiplied by the constant number corresponding to the order of designated signal magnitude.

4. Problem formulation of plate bending and defect detection

The aim of this work is to detect the location of defect provided that the defect (damage) exists in the considered plate structure. The conducted numerical investigation is based on the signal analysis of the structural static and dynamic response. The plate material is assumed as linear-elastic. The plate bending is described and solved by the Boundary Element Method in the direct simplified approach where there is no need to introduce either concentrated forces at the plate corners or equivalent shear forces at the plate continuous edges. This approach is described for static, dynamic and stability analysis in [9, 10]. The static fundamental solution (the Green function) for an infinite plate is used

$$(4.1) \qquad w^*(r) = \frac{1}{8\pi D} r^2 \ln(r),$$

which is the solution of the biharmonic equation:

$$(4.2) \qquad \nabla^4 w^*(r) = \frac{1}{D} \delta(r).$$

For a thin isotropic plate, where $D = Eh^3/(12(1-v^2))$ is the plate stiffness, h is the plate thickness, E and v are the Young modulus and the Poisson's ratio, $\delta(r)$ is the Dirac delta and $r = \sqrt{x^2 + y^2}$.

4.1. Boundary and boundary-domain integral equations for static and dynamic analysis. Derivation of the set of algebraic equations. Calculation of deflection inside a plate domain

A plate supported on boundary and subjected to the external distributed load q is analysed. The boundary integral equations for static analysis of plates are derived using Bettie's theorem and have the form

$$(4.3) \quad c(\mathbf{x})w(\mathbf{x}) + \int_\Gamma \left[T_n^*(\mathbf{y},\mathbf{x})w(\mathbf{y}) - M_{ns}^*(\mathbf{y},\mathbf{x})\frac{\mathrm{d}w(\mathbf{y})}{\mathrm{d}s} - M_n^*(\mathbf{y},\mathbf{x})\varphi_n(\mathbf{y}) \right] \mathrm{d}\Gamma(\mathbf{y})$$

$$= \int_\Gamma \left[\widetilde{T}_n(\mathbf{y})w^*(\mathbf{y},\mathbf{x}) - M_n(\mathbf{y})\varphi_n^*(\mathbf{y},\mathbf{x}) \right] \mathrm{d}\Gamma(\mathbf{y})$$

$$+ \int_\Omega q(\mathbf{y})w^*(\mathbf{y},\mathbf{x}) \, \mathrm{d}\Omega(\mathbf{y}),$$

$$(4.4) \quad c(\mathbf{x})\varphi_n(\mathbf{x}) + \int_\Gamma \left[\overline{T}_n^*(\mathbf{y},\mathbf{x})w(\mathbf{y}) - \overline{M}_{ns}^*(\mathbf{y},\mathbf{x})\frac{\mathrm{d}w(\mathbf{y})}{\mathrm{d}s} - \overline{M}_n^*(\mathbf{y},\mathbf{x})\varphi_n(\mathbf{y}) \right] \mathrm{d}\Gamma(\mathbf{y})$$

$$= \int_\Gamma \left[\widetilde{T}_n(\mathbf{y})\overline{w}^*(\mathbf{y},\mathbf{x}) - M_n(\mathbf{y})\overline{\varphi}_n^*(\mathbf{y},\mathbf{x}) \right] \mathrm{d}\Gamma(\mathbf{y})$$

$$+ \int_\Omega q(\mathbf{y})\overline{w}^*(\mathbf{y},\mathbf{x})\, \mathrm{d}\Omega(\mathbf{y}),$$

where $w^*(r) = w^*(\mathbf{x},\mathbf{y})$ is the fundamental solution, $\mathbf{x}$ is the source point, $\mathbf{y}$ is the field point and $r = |y - x|$. The coefficient $c(x)$ is taken as: 1, when $\mathbf{x}$ is located inside the plate domain; 0.5, when $\mathbf{x}$ is located on the smooth boundary and 0, when $\mathbf{x}$ is located outside the plate domain.

The second boundary integral Eq. (4.4) can be obtained by replacing the unit concentrated force $P^* = 1$ with the unit concentrated moment $M_n^* = 1$. Such a replacement is equivalent to the differentiation of the first boundary integral Eq. (4.3) with respect to the coordinate n at a point $\mathbf{x}$ belonging to the plate domain and letting this point approach the boundary and assuming n to coincide with the normal to it. The force $\widetilde{T}_n(\mathbf{y})$ can be treated as the equivalent shear force $V_n(\mathbf{y})$ on a fragment of the boundary which is located far from the corner or it plays the role of the corner force $R_n(\mathbf{y})$ which is distributed on a small fragment of the boundary close to the corner. In the case of the free edge we must combine the rotation angle in the tangent direction $\varphi_s(\mathbf{y})$ with the fundamental function $M_{ns}^*(\mathbf{y})$. Since the relation between $\varphi_s(\mathbf{y})$ and the deflection is known: $\varphi_s(\mathbf{y}) = \mathrm{d}w(\mathbf{y})/\mathrm{d}s$, the angle of rotation $\varphi_s(\mathbf{y})$ can be evaluated while using a finite difference scheme to the deflection with two or more adjacent nodal values [9, 10]. In this analysis, the employed finite difference scheme includes the deflections of three adjacent nodes [10].

The set of algebraic equations has the form:

$$(4.5) \qquad \begin{bmatrix} \mathbf{G}_{\mathrm{BB}} & \mathbf{G}_{\mathrm{BS}} \\ \boldsymbol{\Delta} & -\mathbf{I} \end{bmatrix} \begin{Bmatrix} \mathbf{B} \\ \varphi_{\mathrm{S}} \end{Bmatrix} = \begin{Bmatrix} \mathbf{F}_{\mathrm{B}} \\ \mathbf{0} \end{Bmatrix},$$

where $\mathbf{G}_{\mathrm{BB}}$ and $\mathbf{G}_{\mathrm{BS}}$ are the matrices of the dimension $(2N \times 2N)$ and $(2N \times S)$, grouping boundary integrals depending on type of boundary respectively, $\boldsymbol{\Delta}$ is the matrix grouping difference operators connecting angles of rotations in the tangent direction with deflections of suitable boundary nodes if the plate has a free edge, N is the number of boundary physical nodes (boundary element of the constant type) and S is the number of boundary physical nodes (boundary elements of the constant type) along the free edge, finally $\mathbf{F}_{\mathrm{B}}$ is the right-hand-side loading vector. In the current numerical analysis, the constant type of element will be used.

The solution of the set of Eq. (4.5) allows to determine suitable boundary variables. Now, using the boundary integral Eq. (4.3) directly and assuming the value of the coefficient $c(\mathbf{x})$ equal to one it is possible to calculate deflection inside the plate domain, which can be expressed as the sum:

$$(4.6) \qquad w(\mathbf{x}) = w\left(\mathbf{B}, \varphi_{\mathrm{S}}\right) + w(p).$$

For the dynamic analysis the boundary and domain integral equations are derived using Betti's theorem, too. Plates supported on boundary and rested on internal column supports will be considered. Inside the plate domain there are additional collocation points introduced which are associated with lumped masses according to the Bèzine technique [17]. In each internal collocation point vectors of displacement $w_i(t)$, acceleration $\ddot{w}_i(t)$ and inertial force $B_i(t)$ dependent on time t are established

$$w_i(t) = W_i \sin \omega\, t,$$
$$(4.7) \qquad \ddot{w}_i(t) = -\omega^2 W_i \sin \omega\, t,$$
$$B_i(t) = B_i \sin \omega\, t,$$

where ω is the natural frequency, and amplitudes of inertial forces are described as:

$$(4.8) \qquad B_i = \omega^2 m_i W_i.$$

The boundary-domain integral equations have the character of amplitude equations [8, 9]:

$$(4.9) \quad c(\mathbf{x})w(\mathbf{x}) + \int\limits_{\Gamma} \left[T_n^*(\mathbf{y},\mathbf{x})w(\mathbf{y}) - M_{ns}^*(\mathbf{y},\mathbf{x})\frac{\mathrm{d}w(\mathbf{y})}{\mathrm{d}s} - M_n^*(\mathbf{y},\mathbf{x})\varphi_n(\mathbf{y}) \right] \mathrm{d}\Gamma(\mathbf{y})$$

$$= \int\limits_{\Gamma} \left[\widetilde{T}_n(\mathbf{y})w^*(\mathbf{y},\mathbf{x}) - M_n(\mathbf{y})\varphi_n^*(\mathbf{y},\mathbf{x}) \right] \mathrm{d}\Gamma(\mathbf{y})$$

$$- \int\limits_{\Omega_r} q_r w^*(r,\mathbf{x})\, \mathrm{d}\Omega_r + \sum_{i=1}^{I} B_i w^*(i,\mathbf{x}),$$

$$(4.10) \quad c(\mathbf{x})\varphi_n(\mathbf{x}) + \int\limits_{\Gamma} \left[\overline{T}_n^*(\mathbf{y},\mathbf{x})w(\mathbf{y}) - \overline{M}_{ns}^*(\mathbf{y},\mathbf{x})\frac{\mathrm{d}w(\mathbf{y})}{\mathrm{d}s} - \overline{M}_n^*(\mathbf{y},\mathbf{x})\varphi_n(\mathbf{y}) \right] \mathrm{d}\Gamma(\mathbf{y})$$

$$= \int\limits_{\Gamma} \left[\widetilde{T}_n(\mathbf{y})\overline{w}^*(\mathbf{y},\mathbf{x}) - M_n(\mathbf{y})\overline{\varphi}_n^*(\mathbf{y},\mathbf{x}) \right] \mathrm{d}\Gamma(\mathbf{y})$$

$$- \int\limits_{\Omega_r} q_r \overline{w}^*(r,\mathbf{x})\, \mathrm{d}\Omega_r + \sum_{i=1}^{I} B_i \overline{w}^*(i,\mathbf{x}).$$

After discretization of the plate boundary using constant type of elements, the set of algebraic equations can be obtained in matrix notation [9, 10]

$$
(4.11) \quad
\begin{bmatrix}
\mathbf{G}_{\mathrm{BB}} & \mathbf{G}_{\mathrm{BS}} & \mathbf{G}_{\mathrm{BR}} & -\lambda \mathbf{G}_{\mathrm{Bw}}\mathbf{M}_{\mathrm{p}} \\
\boldsymbol{\Delta} & -\mathbf{I} & 0 & 0 \\
\mathbf{G}_{\mathrm{RB}} & \mathbf{G}_{\mathrm{RS}} & \mathbf{G}_{\mathrm{RR}} & -\lambda \mathbf{G}_{\mathrm{Rw}}\mathbf{M}_{\mathrm{p}} \\
\mathbf{G}_{\mathrm{wB}} & \mathbf{G}_{\mathrm{wS}} & \mathbf{G}_{\mathrm{wR}} & -\lambda \mathbf{G}_{\mathrm{ww}}\mathbf{M}_{\mathrm{p}}+\mathbf{I}
\end{bmatrix}
\begin{Bmatrix}
\widetilde{\mathbf{B}} \\
\widetilde{\varphi}_s \\
\widetilde{\mathbf{R}} \\
\widetilde{\mathbf{w}}
\end{Bmatrix}
=
\begin{Bmatrix}
\mathbf{0} \\
\mathbf{0} \\
\mathbf{0} \\
\mathbf{0}
\end{Bmatrix},
$$

where $\mathbf{G}_{\mathrm{BR}}$ is the matrix of the dimension $(2N \times R)$ grouping integrals of the fundamental function w^* over the column cross-section; $\mathbf{G}_{\mathrm{Bw}}$ is the matrix of the dimension $(2N \times M)$ grouping values of fundamental function w^* established at the internal collocation points, where M is the number of the internal collocation points and N is the number of the boundary nodes; $\mathbf{G}_{\mathrm{RB}}$ and $\mathbf{G}_{\mathrm{RS}}$ are the matrices of the dimension $(R \times 2N)$ and $(R \times S)$ respectively, grouping boundary integrals; $\mathbf{G}_{\mathrm{RR}}$ is the matrix of the dimension $(R \times R)$ grouping integrals of fundamental function w^* over the column cross-section; $\mathbf{G}_{\mathrm{Rw}}$ is the matrix of the dimension $(R \times M)$ grouping values of fundamental function w^* established at internal collocation points; $\mathbf{G}_{\mathrm{wB}}$ is the matrix of the dimension $(M \times 2N)$ grouping the boundary integrals of the appropriate fundamental functions (depending on type of boundary); $\mathbf{G}_{\mathrm{wS}}$ is the matrix of the dimension $(M \times S)$ grouping the boundary integrals of the appropriate fundamental functions; $\mathbf{G}_{\mathrm{wR}}$ is the matrix of the dimension $(M \times R)$ grouping integrals of fundamental function w^* over the column cross-section; $\mathbf{G}_{\mathrm{ww}}$ is the matrix of the dimension $(M \times M)$ grouping the values of fundamental function w^* established at internal collocation points, R is the number of internal column supports, finally $\mathbf{M}_{\mathrm{p}} = \mathrm{diag}\,(m_1, m_2, m_3, ..., m_M)$ is the plate mass matrix, $\lambda = \omega^2$ and $\mathbf{I}$ is the unit matrix (M is the number of lumped masses). The definition presented above are explained in the Fig. 5 for static and 5b for dynamic analysis [10].
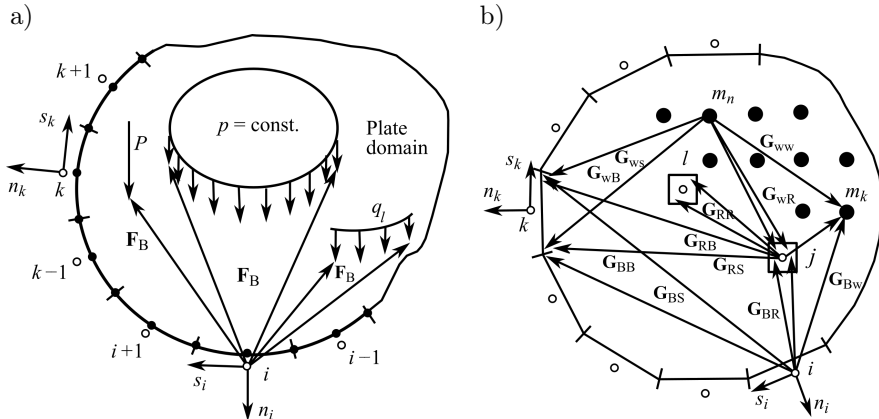

Fig. 5. Vector (a) and matrix (b) designation occurring in Eqs (4.5) and (4.11).

Elimination of boundary variables $\mathbf{B}$ and φ_{S} from the matrix Eq. (4.11) leads to the standard eigenvalue problem

$$(4.12) \qquad \left\{ \mathbf{A} - \widetilde{\lambda}\,\mathbf{I} \right\} \widetilde{\mathbf{w}} = \mathbf{0},$$

wherein $\widetilde{\lambda} = 1/\lambda = 1/\omega^2$,

$$(4.13) \qquad \mathbf{A} = \left(\mathbf{C}_{\mathrm{wB}} \mathbf{C}_{\mathrm{BB}}^{-1} \mathbf{C}_{\mathrm{Bw}} - \mathbf{C}_{\mathrm{ww}} \right) \mathbf{M}_{\mathrm{p}}$$

and

$$(4.14) \qquad \begin{aligned} \mathbf{C}_{\mathrm{BB}} &= \mathbf{G}_{\mathrm{BB}} + \mathbf{G}_{\mathrm{BS}}\boldsymbol{\Delta} - \mathbf{G}_{\mathrm{BR}}\mathbf{G}_{\mathrm{RR}}^{-1}\left(\mathbf{G}_{\mathrm{RB}} + \mathbf{G}_{\mathrm{RS}}\boldsymbol{\Delta}\right), \\ \mathbf{C}_{\mathrm{Bw}} &= \mathbf{G}_{\mathrm{BR}}\mathbf{G}_{\mathrm{RR}}^{-1}\mathbf{G}_{\mathrm{Rw}} - \mathbf{G}_{\mathrm{Bw}}, \\ \mathbf{C}_{\mathrm{wB}} &= \mathbf{G}_{\mathrm{wB}} + \mathbf{G}_{\mathrm{wS}}\boldsymbol{\Delta} - \mathbf{G}_{\mathrm{wR}}\mathbf{G}_{\mathrm{RR}}^{-1}\left(\mathbf{G}_{\mathrm{RB}} + \mathbf{G}_{\mathrm{RS}}\boldsymbol{\Delta}\right), \\ \mathbf{C}_{\mathrm{ww}} &= \mathbf{G}_{\mathrm{wR}}\mathbf{G}_{\mathrm{RR}}^{-1}\mathbf{G}_{\mathrm{Rw}} - \mathbf{G}_{\mathrm{ww}}. \end{aligned}$$

4.2. Modeling of defects in plate boundary and the response signal of the structure

It is assumed, that defects exist near the plate boundary. In other words defects can be modeled as additional plate edges forming a gap (Fig. 6). The boundary conditions assumed for these edges are the same as for a free edge.
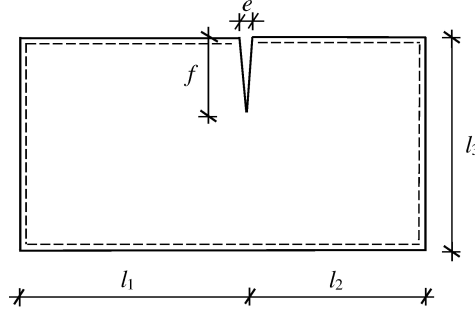
FIG. 6. A plate with damaged edge.

The solution of the set of Eq. (4.5) for static and calculation of deflection, angle of rotation in any directions, bending moments and torsional moments or transverse forces inside a plate domain allow to obtain the response signal of the considered plate structure for DWT analysis. Similarly, the solution of the standard eigenvalue problem described by the relation (4.12), gives eigenvalues as natural vibration frequencies and eigenvectors as deflections at internal collocation points. Furthermore, using the modal analysis it is possible to obtain modes of forced vibration, which can be treated as the structural response for DWT signal analysis.

5. NUMERICAL EXAMPLES

The rectangular plates supported on boundary and resting on internal column supports are considered. Defects are introduced by the additional edges forming slots in the basic plate domain. The BEM is applied to solve a thin plate bending problem. Each plate edge is divided into 30 boundary elements of the constant type. For the supported edges, collocation points are located exactly on elements, for free edges slightly outside the plate boundary as defined by the parameter $\varepsilon = \delta/d$, where δ is the real distance of a collocation point from a plate edge and d is the element length. For each example $\varepsilon = 0.001$ is assumed. Diagonal boundary terms in the characteristic matrix are calculated analytically and remaining ones – using 12-point Gauss quadrature [10]. Plates are subjected to static or dynamic loading. Decomposition of the obtained signal is carried out using DWT with Daubechies 4, 6 8, Coiflet 4, 6 and B-spline 1 families of wavelets. For a selected example the white noise was introduced, too.

5.1. *Two-dimensional analysis of static response signal*

The square plate supported on boundary and subjected to static uniformly distributed load $p = 5$ kN/m^2 is considered and presented in Fig. 7. The plate properties are $E = 30.0$ GPa, $v = 0.16$ and the plate thickness is $h = 0.1$ m. In the middle of one edge the slot has been introduced symmetrically and described by the parameter $e = 0.01$ (Fig. 7). External loading p is applied on the left-hand half of the plate domain.
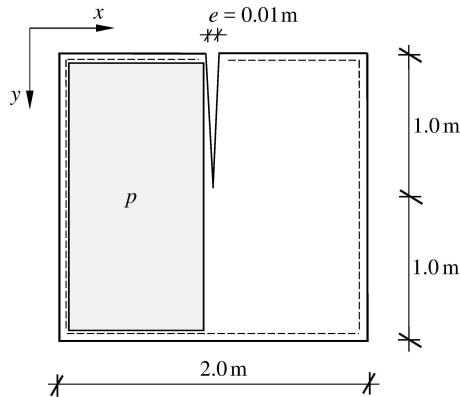
FIG. 7. The square plate subjected to uniformly distributed loading p.

Two-dimensional DWT analysis in the field of x and y has been carried out. The two-dimensional set of measurement points with regular localization inside of the plate domain was prepared. The number of measurements in two perpendicular directions is $N_x = N_y = 64$. The static vertical displacements were

registered as the signal for decomposition. The results of calculation with the use of Coiflet 4 wavelet are presented in Fig. 8 and B-spline 1 wavelet in Fig. 9. In both cases the presence as well as the location of the crack were well exposed. However, one must be aware of the existence of the boundary disturbances, not necessarily connected with the existence of a defect in this particular place.
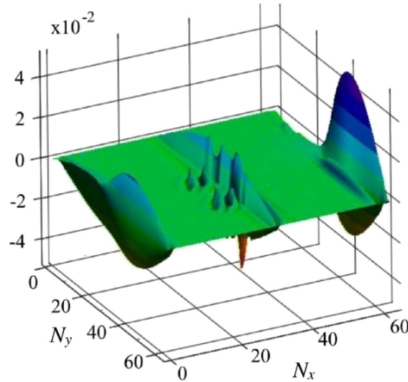

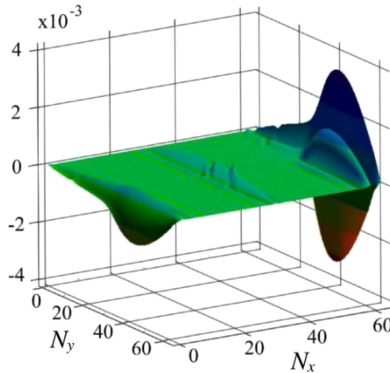FIG. 8. 2-D DWT (Coiflet 4, detail 1) signal: vertical displacements, $N_x = N_y = 64$ – number of measurements.

FIG. 9. 2-D DWT (B-spline 1, detail 1) signal: vertical displacements, $N_x = N_y = 64$ – number of measurements.

5.2. One-dimensional analysis of dynamic response signal

Example 1. Rectangular plate resting on eight internal column supports is considered and presented in Fig. 10. Two parameters d and e describe dimension of a crack located near one plate edge. The crack dimensions are also presented in Fig. 10. It is assumed, that plate deformations according to first four modes of vibration are taken as the plate response signals. The number of measurements is $N = 64$. The results of calculation for the first two modes registered along
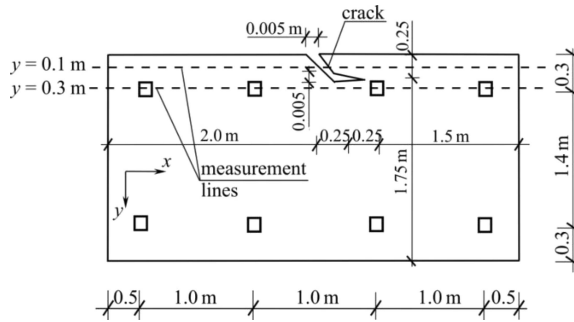
FIG. 10. Rectangular plate resting on eight internal column supports.

the line with the distance $y = 0.1$ m from the longer edge are presented in Fig. 11. In both cases the presence and the location of damage were properly indicated by the high peaks of the transformed signal. Decomposition of the similar signal, i.e. amplitude displacements for the first and second mode yet measured along the line with the distance $y = 0.3$ m has also revealed the existence and position of the crack (Figs 11, 12). Moreover, in the Fig. 12b one can estimate the extent of the defect. Worth noting is the fact that the presence of internal supports/columns does not disrupt the correct damage detection.
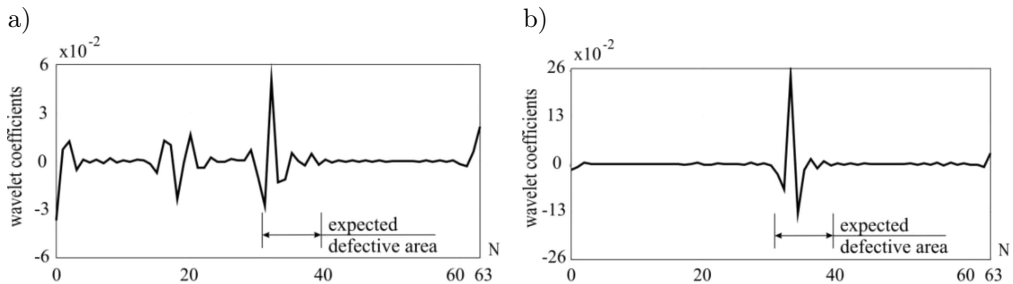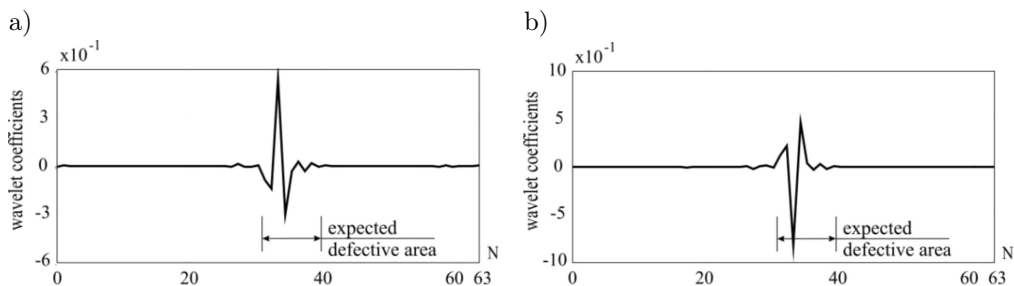

FIG. 11. 1-D DWT (Daubechies 6, detail 1) signal: vertical displacements according to the first (a) and the second (b) modes of vibration, $y = 0.1$ m, $N = 64$ – number of measurements.
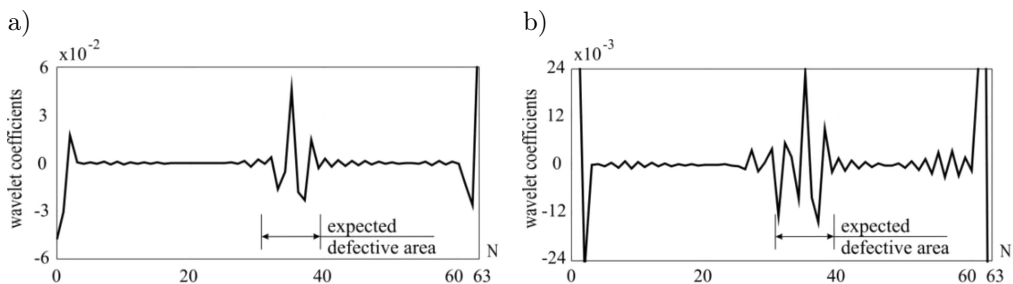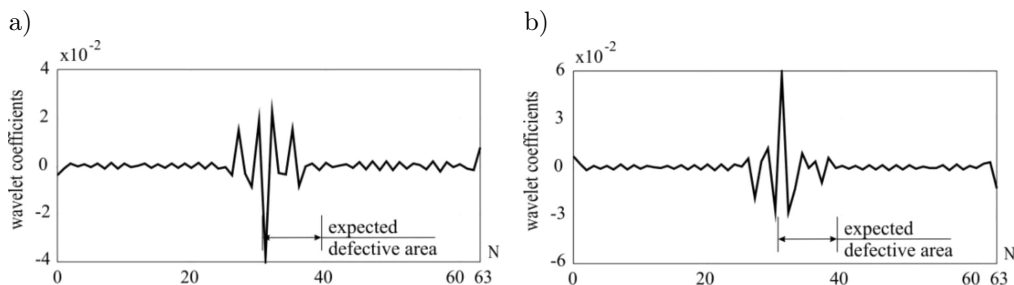

FIG. 12. 1-D DWT (Daubechies 4, detail 1) signal: vertical displacements according to the first (a) and the second (b) modes of vibration, $y = 0.3$ m, $N = 64$ – number of measurements.

Example 2. Rectangular plate resting on two opposite edges and four column supports is considered and presented in Fig. 13. The analyses have been performed for the data set in the form of amplitudes of vertical displacements for the third and fourth mode measured in 64 points along the line with the distance $y = 0.1$ m and $y = 0.3$ m, respectively. The results of signal decomposition, presented in Figs 14 and 15, revealed the existence and location of the crack. Noteworthy is the fact that amended terms of support when compared to Example 1 caused smaller boundary disturbances in the transformation window.
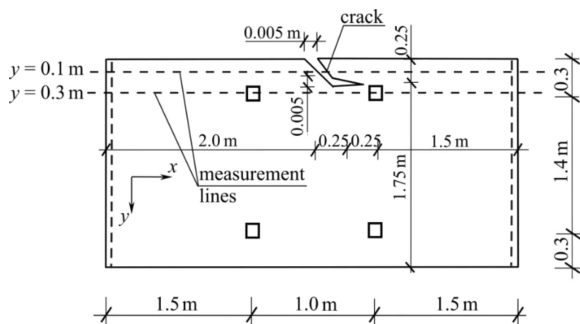
FIG. 13. Rectangular plate resting on two opposite edges and four column supports.

a)

b)

FIG. 14. 1-D DWT (Daubechies 4, detail 1) signal: vertical displacements according to the third (a) and fourth (b) modes of vibration, $y = 0.1$ m, $N = 64$ – number of measurements.
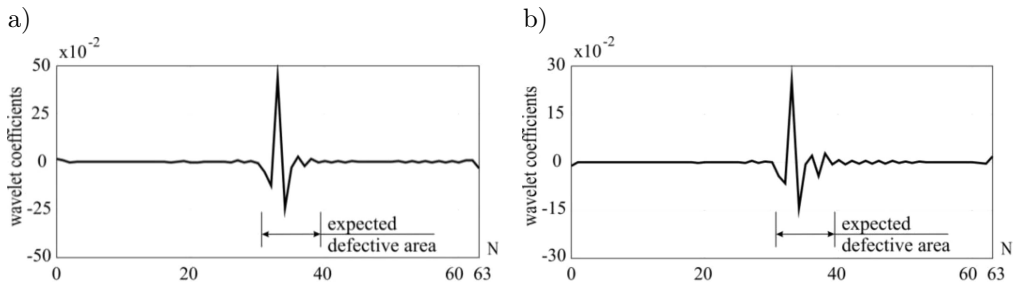
a)

b)

FIG. 15. 1-D DWT (Daubechies 4, detail 1) signal: vertical displacements according to the third (a) and the fourth (b) modes of vibration, $y = 0.3$ m, $N = 64$ – number of measurements.

Example 3. Rectangular plate supported at all four corners and resting on four column supports is considered and presented in Fig. 16. DWT has been conducted for the signal of vertical displacement amplitudes for the second and third mode, measured in 64 points along the line with the distance $y = 0.1$ m and $y = 0.3$ m. In Figs 17 and 18 the presence and the position of the defect can be noted by the means of evident high peaks. In the case of the structural response signal registered along the line with the distance $y = 0.3$ m the width
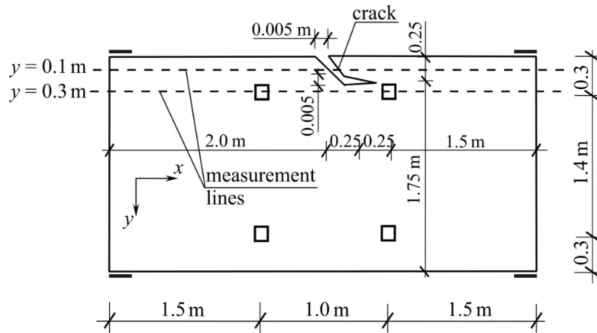
FIG. 16. Rectangular plate supported in four corners and resting on four column supports.

FIG. 17. 1-D DWT (Daubechies 4, detail 1) signal: vertical displacements according to the second (a) and the third (b) modes of vibration, $y = 0.1$ m, $N = 64$ – number of measurements.
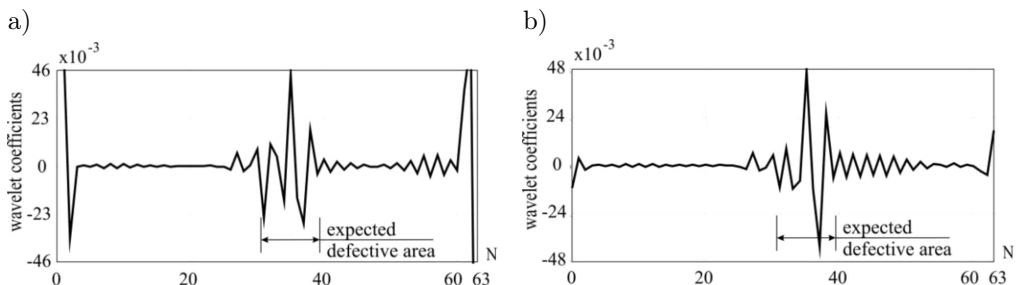

FIG. 18. 1-D DWT (Daubechies 4, detail 1) signal: vertical displacements according to the second (a) and the third (b) modes of vibration, $y = 0.3$ m, $N = 64$ – number of measurements.

of disturbances area is greater (Fig. 18) when compared to the results for the distance $y = 0.1$ m (Fig. 17) and corresponds to the length of the crack.

Example 4. Plate presented in Fig. 16 is considered. The analysis has been performed for the vertical displacements according to the third mode of vibration, the measurement line distance $y = 0.1$ m. The randomly generated white noise was introduced with the maximum intensity 30% of the response signal measured value (relative to the highest measured value). For the signal decomposition Daubechies 4 and 8 families of wavelets were applied. Despite previous experience [12] which revealed that the damage is in fact unidentifiable for the noise level higher than 5% in this case the crack presence was revealed for the 20 % noise level. DWT, details 1 are presented in Figs. 19bc. The obtained results give hope for the application of the method in detecting defects during real experiments for contaminated data.
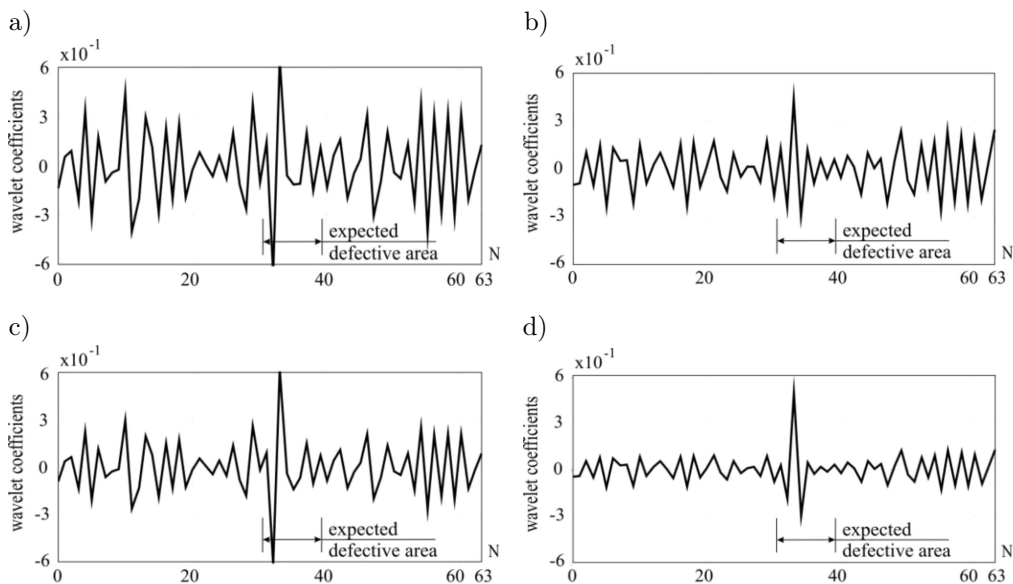

FIG. 19. 1-D DWT (detail 1) signal: vertical displacements according to the third mode of vibration, Daubechies 8, noise 30%: a) Daubechies 4, noise 20%, b) Daubechies 8, noise 20%, c) Daubechies 4, noise 10%, d) $y = 0.1$ m, $N = 64$ – number of measurements.

5.3. Two-dimensional analysis of dynamic response signal

Rectangular plate simply-supported on two opposite edges is considered and presented in Fig. 20. The plate properties are $E = 30.0$ GPa, $v = 0.16$ and the plate thickness is $h = 0.1$ m. In the middle of one edge the slot has been introduced symmetrically and described by the parameter $e = 0.008$ m. The analysis has been performed for the vertical displacements according to the first,
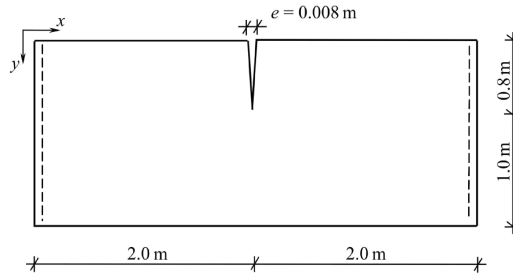
Fig. 20. Rectangular plate simply-supported on two opposite edges.

third and fourth mode of vibration, measured in two-dimensional domain of 64×64 points, which form the regular grid. The results of calculation with the use of B-spline 1, Coiflet 6 and Daubechies 6 wavelet are presented in Figs 21, 22, and 23, respectively. In all the cases the presence and the location of the crack were well exposed.
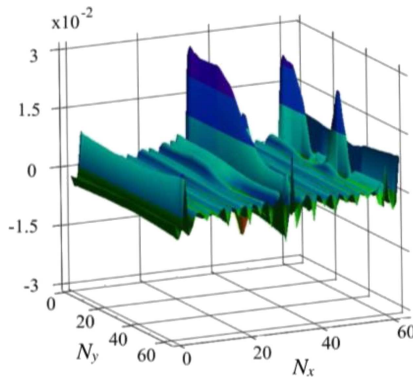

Fig. 21. 2-D DWT (B-spline 1, detail 1) signal: vertical displacements, mode 1, $N_x = N_y = 64$ – number of measurements.
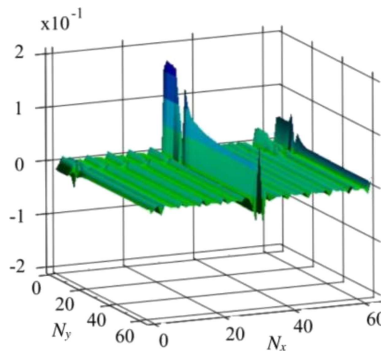

Fig. 22. 2-D DWT (Coiflet 6, detail 1) signal: vertical displacements, mode 3, $N_x = N_y = 64$ – number of measurements.
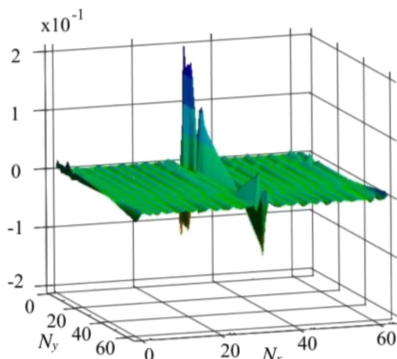
Fig. 23. 2-D DWT (Daubechies 6, detail 1) signal: vertical displacements, mode 4, $N_x = N_y = 64$ – number of measurements.

6. Concluding remarks

Application of discrete 1-D and 2-D wavelet transformation (DWT) to recognition of structural response signal discontinuity in the analysis of plates is discussed in the paper. Considered plates are supported on boundary or by internal columns. The thin (Kirchhoff) plate bending is described by the boundary-domain integral equations and solved while using the Boundary Element Method (BEM). Numerical analysis of the structure by the BEM, by which the signal of structural response is obtained replaces experimental data. All defects are introduced by additional edges forming slots or holes in the relation to the basic plate domain. Measured response signal was assumed as the static deflection surface for 2-D and modes of vibrations for 1-D discrete wavelet transform, respectively. To make the values of the structure response signal more realistic, the white noise disturbing signal was additionally introduced and considered in selected examples. Damage was properly localized while using asymmetric Daubechies 4, 6, 8 set of wavelets as well as nearly symmetrical Coiflet 6 and B-spline 1 set of wavelets in signal decomposition. The position of defects was quite correctly identified by the high peak of the transformed data. The detection of defects localized inside the plate domain was not considered in this paper. The minimum number of measurements was assumed as sixty four.

References

1. Mróz Z., Garstecki A., Optimal loading conditions in design and identification of structures. Part 1: Discrete formulation, *International Journal of Structural and Multidisciplinary Optimization*, **29**: 11–18, 2005.

2. DEMS K., MRÓZ Z., Identification of damage in beam and plate structures using parameter dependent frequency changes, *Engineering Computation*, **18**(1/2): 96–120, 2001.

3. ZIOPAJA K., POZORSKI Z., GARSTECKI A., Damage detection using thermal experiments and wavelet transformation, *Inverse Problems in Science and Engineering*, **19**(1): 127–153, 2011.

4. BOUMECHRA N., Damage detection in beam and truss structures by the inverse analysis of the static response due to moving loads, *Structural Control Health Monitoring*, **24**(10): 1972, 2017, doi.org/10.1002/stc.1972.

5. KNITTER-PIATKOWSKA A., GARBOWSKI T., Damage detection through wavelet decomposition and soft computing, [in:] *Proceedings of International Conference on Adaptive Modeling and Simulation ADMOS 2013, Lisbon, Portugal, June 3–5, 2013*, J.P. Moitinho de Almeida, P. Díez, C. Tiago, N. Parés [Eds] , pp. 389–400, CIMNE Barcelona, 2013.

6. WANG Q., DENG X., Damage detection with spatial wavelets, *Journal of Solids and Structures*, **36**: 3443–3468, 1999.

7. KNITTER-PIĄTKOWSKA A., GUMINIAK M., Defect detection in plate structures using wavelet transformation, *Engineering Transactions*, **64**(2): 139–156, 2016.

8. AN Y, CHATZI E, SIM S-H, LAFLAMME S, BLACHOWSKI B, OU J., Recent progress and futuretrends on damage identification methods for bridge structures, *Structural Control Health Monitoring*, **26**: e2416, 2019, https://doi.org/10.1002/stc.2416.

9. GUMINIAK M., Static and Free Vibration Analysis of Thin Plates of the Curved Edges by the Boundary Element Method Considering an Alternative Formulation of Boundary Conditions, *Engineering Transactions*, **64**(1): 3–32, 2016.

10. GUMINIAK M., *The Boundary Element Method in plate analysis* [in Polish], Poznan University of Technology Publishing House, Poznań 2016.

11. KNITTER-PIĄTKOWSKA A., GUMINIAK M., HLOUPIS G., Crack identification in plates using 1-D discrete wavelet transform, *Journal of Theoretical and Applied Mechanics*, **55**(2): 481–496, 2017.

12. GUMINIAK M., KNITTER-PIĄTKOWSKA A., Selected problems of damage detection in internally supported plates using one-dimensional Discrete Wavelet Transform, *Journal of Theoretical and Applied Mechanics*, **56**(2): 631–644, 2018.

13. MALLAT S.G., A theory for multiresolution signal decomposition: The wavelet representation, *IEEE Transactions on Pattern Analysis and Machine Intelligence*, **11**(7): 674–693, 1998.

14. KNITTER-PIĄTKOWSKA A., *Application of Wavelet Transform to detect damage in statically and dynamically loaded structures* [in Polish], Poznan University of Technology Publishing House, Poznań 2011.

15. DOBRZYCKI A., MIKULSKI S., Using of continuous wavelet transform for de-noising signals accompanying electrical treeing in epoxy resins, *Przegląd Elektrotechniczny* (*Electrotechnical Review*), **92**(4): 26–29, 2016, doi: 10.15199/48.2016.04.07.

16. Dodge Y., *The Oxford Dictionary of Statistical Terms*, Oxford University Press, 2003.

17. Bèzine G., Gamby D.A., A new integral equations formulation for plate bending problems, *Advances in Boundary Element Method*, Pentech Press, London, 1978.